Net landscape carbon balance of a tropical savanna: Relative importance of fire and aquatic export in offsetting terrestrial production

10 authors, including:

Clément Duvert
Charles Darwin University
34 PUBLICATIONS **567** CITATIONS

SEE PROFILE

Lindsay B. Hutley
Charles Darwin University
235 PUBLICATIONS **8,723** CITATIONS

SEE PROFILE

Michael I Bird
James Cook University
384 PUBLICATIONS **17,714** CITATIONS

SEE PROFILE

Christian Birkel
University of Costa Rica
162 PUBLICATIONS **2,438** CITATIONS

SEE PROFILE

Some of the authors of this publication are also working on these related projects:

Project — Systematic review for carbon stock and flux in mangrove ecosystems associated with land-use and land-cover change View project

Project — The consequences of mangrove dieback on the coastal carbon cycle View project

PRIMARY RESEARCH ARTICLE

Global Change Biology　WILEY

Net landscape carbon balance of a tropical savanna: Relative importance of fire and aquatic export in offsetting terrestrial production

Clément Duvert[1] ￼ | Lindsay B. Hutley[1] ￼ | Jason Beringer[2] ￼ | Michael I. Bird[3] ￼ | Christian Birkel[4,5] ￼ | Damien T. Maher[6] ￼ | Matthew Northwood[1] | Mitchel Rudge[7] ￼ | Samantha A. Setterfield[8] ￼ | Jonathan G. Wynn[9] ￼

[1]Research Institute for the Environment & Livelihoods, Charles Darwin University, Darwin, NT, Australia

[2]School of Agriculture & Environment, The University of Western Australia, Perth, WA, Australia

[3]College of Science & Engineering, James Cook University, Cairns, Qld, Australia

[4]Department of Geography, Water & Global Change Observatory, University of Costa Rica, San José, Costa Rica

[5]Northern Rivers Institute, University of Aberdeen, Aberdeen, UK

[6]Southern Cross Geoscience, Southern Cross University, Lismore, NSW, Australia

[7]Sustainable Minerals Institute, The University of Queensland, Brisbane, Qld, Australia

[8]School of Biological Sciences, The University of Western Australia, Perth, WA, Australia

[9]Division of Earth Sciences, National Science Foundation, Alexandria, VA, USA

Correspondence
Clément Duvert, Research Institute for the Environment & Livelihoods, Charles Darwin University, Darwin, NT, Australia.
Email: clem.duvert@cdu.edu.au

Abstract

The magnitude of the terrestrial carbon (C) sink may be overestimated globally due to the difficulty of accounting for all C losses across heterogeneous landscapes. More complete assessments of net landscape C balances (NLCB) are needed that integrate both emissions by fire and transfer to aquatic systems, two key loss pathways of terrestrial C. These pathways can be particularly significant in the wet–dry tropics, where fire plays a fundamental part in ecosystems and where intense rainfall and seasonal flooding can result in considerable aquatic C export (ΣF_{aq}). Here, we determined the NLCB of a lowland catchment (~140 km^2) in tropical Australia over 2 years by evaluating net terrestrial productivity (NEP), fire-related C emissions and ΣF_{aq} (comprising both downstream transport and gaseous evasion) for the two main landscape components, that is, savanna woodland and seasonal wetlands. We found that the catchment was a large C sink (NLCB 334 Mg C km^{-2} year^{-1}), and that savanna and wetland areas contributed 84% and 16% to this sink, respectively. Annually, fire emissions (−56 Mg C km^{-2} year^{-1}) and ΣF_{aq} (−28 Mg C km^{-2} year^{-1}) reduced NEP by 13% and 7%, respectively. Savanna burning shifted the catchment to a net C source for several months during the dry season, while ΣF_{aq} significantly offset NEP during the wet season, with a disproportionate contribution by single major monsoonal events—up to 39% of annual ΣF_{aq} was exported in one event. We hypothesize that wetter and hotter conditions in the wet–dry tropics in the future will increase ΣF_{aq} and fire emissions, potentially further reducing the current C sink in the region. More long-term studies are needed to upscale this first NLCB estimate to less productive, yet hydrologically dynamic regions of the wet–dry tropics where our result indicating a significant C sink may not hold.

KEYWORDS

carbon dioxide, fire-related emissions, fluvial carbon transport, inland waters, land carbon sink, methane, net ecosystem carbon budget, seasonal wetland

1 | INTRODUCTION

Globally, terrestrial ecosystems are a net sink for atmospheric carbon dioxide (CO_2), yet the magnitude of this sink remains uncertain, principally because not all carbon (C) losses are accurately accounted for in C budgets (Chapin et al., 2006; Kirschbaum, Zeng, Ximenes, Giltrap, & Zeldis, 2019). Uncertainty is especially large in the tropics where emissions from ecosystem disturbances such as fire can considerably diminish the strength of the terrestrial C sink (van der Werf et al., 2010). Terrestrial C budgets are impacted by fire via the direct combustion of primary productivity but also via the C cost of post-fire regrowth and recovery (Chuvieco, 2009). Global fire emissions are estimated at 2.2 Pg C/year (van der Werf et al., 2017), a flux of similar magnitude to the net terrestrial C sink (Friedlingstein et al., 2019). At regional to catchment scales, estimating C emissions from fire is uncertain, driven largely by inaccurate detection of burnt area at fine scales (<250 m), spatial variability of combustion completeness and interannual variability of fuel production (van der Werf et al., 2017).

Another pathway that has potential to significantly offset the magnitude of the terrestrial C sink is the aquatic export of terrestrial C (Billett et al., 2004; Butman et al., 2016; Kling, Kipphut, & Miller, 1991; Raymond et al., 2013), hereafter abbreviated as ΣF_{aq} to reflect the sum of exports from inland waters, including downstream flux (dissolved inorganic carbon [DIC]; dissolved organic carbon [DOC]; particulate organic carbon [POC]) and gaseous evasion (CO_2; methane [CH_4]). According to recent estimates, ΣF_{aq} may be as high as 5.1 Pg C/year globally (Drake, Raymond, & Spencer, 2018), larger than the global net terrestrial C sink. Recent work based on continental and global datasets suggests that ΣF_{aq} tends to scale with the terrestrial net ecosystem productivity (NEP) of a given catchment (Butman et al., 2016; Webb, Santos, Maher, & Finlay, 2019). However, these studies also highlight considerable variability in the relationship of ΣF_{aq} to NEP across ecosystems, and to date accounting for the role of ΣF_{aq} in offsetting NEP remains elusive. The lack of sufficient site-specific observations that integrate terrestrial and aquatic C fluxes is preventing a full understanding of the significance of and controls on ΣF_{aq} (Webb et al., 2019), which, in turn, hinders our ability to accurately evaluate catchment- and landscape-scale C budgets.

Despite the knowledge that tropical freshwaters may contribute disproportionately to global ΣF_{aq}, large observational gaps remain in this region (Aufdenkampe et al., 2011; Drake et al., 2018; Lauerwald, Laruelle, Hartmann, Ciais, & Regnier, 2015; Raymond et al., 2013; Regnier et al., 2013). Few catchment-scale studies explicitly relating ΣF_{aq} to terrestrial NEP have been conducted in the tropics (Davidson, Figueiredo, Markewitz, & Aufdenkampe, 2010; Hastie, Lauerwald, Ciais, & Regnier, 2019; Vihermaa et al., 2016; Waterloo et al., 2006; Zhou et al., 2013). To our knowledge, none have been undertaken in the wet–dry tropics, a vast area comprising ~11% of the global land area (Beck et al., 2018) where highly seasonal rainfall regimes and frequent fire result in considerable variations in C budgets, both spatially and temporally.

Landscapes of the wet–dry tropics are typically composed of various ecosystem types, including dry-deciduous forests, savanna woodlands and seasonal wetlands and floodplain networks. Savannas are among the most fire-prone ecosystems globally (Beringer et al., 2015; van der Werf et al., 2010), while seasonal wetlands are known to play a major role in aquatic C export (Abril & Borges, 2019; Abril et al., 2014; Borges et al., 2015, 2019). These wetlands can also be significantly affected by fire during the drier months (Mitsch et al., 2010). Given the likely large spatial heterogeneities in C budgets between different landscape components, a landscape-scale approach is required for the wet–dry tropics. In this regard, integrative approaches such as those being developed for the boreal biome are of particular interest (Chi et al., 2020; Hutchins, Casas-Ruiz, Prairie, & del Giorgio, 2020; Hutchins, Tank, et al., 2020; Öquist et al., 2014). Here, we use the net landscape C balance (NLCB) approach as introduced by Chi et al. (2020) to account for the diversity in landscape components and their varying contributions to catchment-scale C cycling.

Extremely high fluxes of terrestrially derived, dissolved C have been observed in the tropical savannas of northern Australia (Duvert et al., 2020; Tweed et al., 2016), but how this seasonal aquatic C flux compares to terrestrial productivity remains unknown. Regional and continental-scale C budgets for Australia do not fully account for ΣF_{aq} losses (Beringer et al., 2015; Haverd et al., 2013), with DIC and gaseous evasion from inland waters often overlooked. Northern Australian savannas can lose up to ~50% of NEP to fire (Beringer, Hutley, Tapper, & Cernusak, 2007; Murphy, Prior, Cochrane, Williamson, & Bowman, 2019), and these ecosystems are currently seen as a weak C sink to a C source depending on the extent of fire (Beringer et al., 2015). While the magnitude of ΣF_{aq} is unlikely to be as high as fire-related C loss, inclusion of all offsets to NEP may shift the source–sink status of Australian tropical savannas. With increasing climatic extremes in the region (Herold, Ekström, Kala, Goldie, & Evans, 2018; Jourdain et al., 2013), a thorough understanding of the short- and long-term feedbacks between climate, NEP, fire and ΣF_{aq} is needed (Hastie et al., 2019).

In this study, we aimed to determine the importance of two C loss pathways, namely fire and aquatic C export, and their role in offsetting the terrestrial C sink of a tropical catchment comprised of savanna woodland and seasonal wetlands. To achieve this, we modelled estimates of NEP for the two landscape components constrained by eddy-covariance measurements. We also quantified monthly C losses from fire emissions using a spatially explicit approach based on satellite imagery. To assess ΣF_{aq}, we measured the fluxes of DIC, DOC and POC in river water and estimated the evasion of CO_2 and CH_4 from both the river and wetland surfaces. We then examined how fire and aquatic C losses compared to a landscape-averaged NEP at both annual and monthly time-scales to derive an NLCB (after Chi et al., 2020) for our targeted catchment. The study was conducted over a 2-year period in the Howard River catchment where there is a long-term flux tower site (AU-How) that is part of the Australian flux network, OzFlux (Beringer et al., 2016).

2 | METHODS

2.1 | Study site

The Howard River catchment (~140 km^2) is located in the wet–dry tropics of the Northern Territory, Australia. The low-relief landscape supports savanna woodlands (~35% of the catchment area) as well as permanent wetlands and seasonally inundated floodplains (~23%; Hutley, Beringer, Isaac, Hacker, & Cernusak, 2011; Moore et al., 2018). A zone of peri-urban, rural development occupies the remaining area (~42%) and is dominated by relatively large land parcels (2–5 ha) covered by native savanna vegetation. The savanna woodland NEP measured at AU-How is in the range 350–510 Mg C km^{-2} year^{-1} (Beringer et al., 2007), with fire-related C loss estimated to reduce NEP by 160 Mg C km^{-2} year^{-1} on average depending on intensity and frequency (Beringer et al., 2007). Chen, Hutley, and Eamus (2003) also reported a similar NEP (380 Mg C km^{-2} year^{-1}) based on repeated measures of tree increment, litterfall, soil and stem respiration (Re) in the catchment.

The annual rainfall average for the catchment was 1,890 mm for the period 1989–2018 (see Section 2.5), while annual runoff was 680 mm with large interannual variations. Over 90% of rainfall occurs between November and April, and, at the peak of the wet season, flooded land occupies almost a quarter of the catchment. These wetlands then surficially drain to the river until they dry out around June–July, depending on the magnitude and timing of wet season flooding (Birkel et al., 2020; Duvert et al., 2019). In the dry season, baseflow is sustained by a deep dolomite aquifer (Cook et al., 1998). High fluxes of terrestrially derived DIC and DOC occur during the wet season, which have been related to high connectivity between riparian floodplains, wetlands, shallow groundwater and the stream network (Birkel et al., 2020; Duvert et al., 2020).

2.2 | Quantification of aquatic C export

2.2.1 | Dissolved CO$_2$, DIC and DOC measurements

To quantify the DIC and DOC fluxes exiting the catchment via runoff, and the CO$_2$ flux released from the river system, we measured the dissolved concentrations of DIC, DOC and CO$_2$ in the river at a bi-hourly frequency over a 2-year period. While the DOC and CO$_2$ concentrations were measured directly, the DIC concentrations were obtained indirectly from pCO$_2$, pH and temperature measurements (see details below). The study spanned 2 years from October 2016 to October 2018. In the following, 'year 1' and 'year 2' refer to the water-years October 2016–September 2017 and October 2017–September 2018, respectively.

We used a custom-made equilibration chamber similar to that described in Santos, Maher, and Eyre (2012). Every 2 hr, a small submersible pump (Cyclone, Proactive) drew ~9 L of river water into a sealed chamber where an S-can spectrometer (Messtechnik GmbH) measured DOC, a PHEHT sensor (Ponsel) measured pH (±0.1) and

water temperature (±0.01°C) at the start of each 2-hr cycle. In addition, the chamber headspace was linked to a non-dispersive infrared CO$_2$ sensor (GMP343, Vaisala) via a micropump (NMP-015B, KNF). The headspace air was continuously circulated through a Nafion dryer (MD-070-24P-4, Perma Pure) into the CO$_2$ sensor and back into the bottom of the chamber. Gas equilibration was generally reached in 30–40 min, and pCO$_2$ was recorded 1 hr after sampling. Sensors were connected to a CR3000 datalogger (Campbell Scientific) and powered by a 12V battery recharged by solar panels.

2.2.2 | Sensor calibration

To calibrate our high-frequency monitoring system described above, samples were collected on a weekly to monthly basis for 2 years, resulting in 58 DIC and 31 DOC samples. Briefly, DIC concentrations were quantified using an extraction chamber connected to a Picarro G2101-i (Bass, Bird, Munksgaard, & Wurster, 2012), while DOC concentrations were measured on an organic carbon analyser (Shimadzu TOC-VCPH). The pH probe was calibrated at every site visit (weekly to monthly), while the pCO$_2$ probe was calibrated twice over the course of the experiment using pure N$_2$ gas (zero) and a CALGAZ CO$_2$ standard (10,000 ppm). No significant drift in reported CO$_2$ concentrations was observed. Further details on the DOC and DIC calibration procedures are available in the Supporting Information (Methods S1 and S2).

2.2.3 | POC measurements

To determine the concentration of POC transported in suspended sediment, we also collected 13 samples under a wide range of flow conditions. These POC samples were analysed on a Flash elemental analyser and a Delta V Plus isotope ratio mass spectrometer (Thermo Scientific; see Methods S4 in Supporting Information).

2.2.4 | DIC, DOC and POC load estimates

We derived a time-series of DIC concentrations from our 2-hourly measurements of pCO$_2$, pH and temperature using the CO$_2$ solubility constant from Plummer and Busenberg (1982) and the dissociation constants from Harned and Davis (1943). We then compared the high-frequency DIC values to the DIC measurements obtained from grab samples and used the resultant regression to compute corrected DIC values (Methods S2 in Supporting Information). Annual DIC loads were then estimated from the corrected DIC data and corresponding discharge time-series. Uncertainties on DIC load estimates were quantified using a Monte Carlo error propagation approach (Methods S3 in Supporting Information). Because the catchment is underlain by a dolostone formation, some of the DIC will originate from carbonate weathering. To discard the weathering-sourced DIC, we applied the isotopically derived, seasonally varying

partitioning estimates as reported by Duvert et al. (2020) for the Howard River to estimated daily loads. We also propagated uncertainties on these partitioning estimates.

Similarly, we calibrated the raw sensor DOC time-series using the values obtained from grab samples (Methods S1 in Supporting Information). Annual DOC loads and associated uncertainties were then estimated with the same procedure used to determine DIC (Methods S3 in Supporting Information). Unlike DIC and DOC, POC loads were estimated from a limited number of samples ($n = 13$), which unsurprisingly led to greater uncertainties. In this instance, we chose to use the LOADEST Fortran program (Runkel, Crawford, & Cohn, 2004) to develop a regression model that allowed prediction of POC concentration from discharge data (Methods S4 in Supporting Information). For all load estimates, we provide 95% confidence intervals, that is, the range between percentiles 2.5 and 97.5 ($\approx \pm 2\sigma$).

2.2.5 | Riverine and wetland CO_2 evasion estimates

A large proportion of ΣF_{aq} can occur via the evasion of CO_2 at the water–air interface. We expected emissions from the seasonal wetlands to be controlled by different factors when compared to emissions from the river itself, and therefore we distinguished between these two evasion fluxes in our calculations. For the seasonally flooded areas, CO_2 evasion was directly integrated into wetland NEP estimates based on eddy-covariance flux measurements at a nearby seasonal floodplain (Beringer, Livesley, Randle, & Hutley, 2013; see Section 2.3.2). For the river network, the rate of CO_2 evasion was estimated using three independent methods as detailed below.

The first method (hereafter referred to as 'mass balance') is based on the prior quantification of water source contributions (Duvert et al., 2020). In this instance, the rate of CO_2 evasion was calculated as the sum of CO_2 losses from each water source to the river outlet. The second method ('groundwater recharge') involved indirectly estimating CO_2 evasion by quantifying the flux of DIC recharging the shallow aquifer. This method used the water table fluctuation approach (Healy & Cook, 2002) and required subtracting the downstream export of DIC to avoid double accounting. The third method ('empirical models') involved estimating the gas transfer velocity (k_{CO2}) using the three empirical models with best predictive power from Raymond et al. (2012), and deriving a time-series of the CO_2 evasion flux from k_{CO2} values and our high-frequency pCO_2 measurements. For each of the three methods, uncertainties were estimated via Monte-Carlo simulations. Further details on each method are provided in the Supporting Information (Methods S5). All data analyses were conducted in MATLAB R2017b.

2.2.6 | Riverine and wetland CH_4 evasion estimates

Another potentially significant component of the NLCB is related to CH_4 evasion. For the seasonal wetlands, the evasion of CH_4 was estimated from a seasonal floodplain ~20 km from the Howard River, based on three measurement campaigns covering both flooded and non-flooded conditions (Beringer et al., 2013). Wet season CH_4 fluxes in Beringer et al. (2013) were measured using floating chambers distributed across the major vegetation types of the wetland and include diffusive, ebullitive and plant-mediated fluxes. Because of the geomorphologic, climatic and environmental similarities between this site and the Howard River catchment, we used this previously established flux and scaled it to the area covered by seasonal wetlands in the Howard River catchment. For the river network, we hypothesized that CH_4 evasion would be negligible, an assumption that we later discuss.

2.3 | Quantification of savanna and wetland NEP

To account for the heterogeneities in C sink strength between different ecosystems, we derived NEP estimates for two dominant landscape components, (a) upland and peri-urban savanna and (b) seasonally flooded land. To do this, land use types were grouped using the SCP plugin in QGIS 2.14.3 and maximum likelihood supervised classification of a Sentinel-2A image (European Space Agency) taken in May 2019. The rural development areas (42% of the catchment area) were included in the savanna vegetation type because all the isolated dwellings across the catchment occur within managed native savanna vegetation and do not affect the canopy cover significantly. After all infrastructure (e.g. roofs, road networks) was excluded from these peri-urban areas, the landscape was comprised of ~75% savanna and ~25% seasonally flooded land.

2.3.1 | NEP estimate for the savanna component

To obtain daily, monthly and annual NEP estimates for the savanna component, we acquired half-hourly fluxes of sensible heat, latent heat and net CO_2 at the AU-How site throughout the 2 years of riverine measurements. Briefly, flux instruments are mounted on a 23 m guyed mast with adequate homogeneous fetch in all directions (~0.7 to 1.5 km) and slopes of <1. The instrumentation consists of a CSAT3 three-dimensional ultrasonic anemometer (Campbell Scientific) and an LI-7500 open path CO_2/H_2O analyser (Licor). Further details about the experimental setup at this long-term flux tower can be found in Beringer et al. (2007) and Hutley and Beringer (2011). Data were quality-controlled, gap-filled and NEP partitioned into gross primary production (GPP) and Re using the OzFluxQC and DINGO suites of Python scripts (Beringer, McHugh, Hutley, Isaac, & Kljun, 2017; Isaac et al., 2017). Further details on the procedure used to process eddy covariance data are given in the Supporting Information (Methods S6). As Livesley et al. (2011) have previously shown, CH_4 fluxes from the savanna environment are negligible relative to the magnitude of CO_2 fluxes; hence, we decided to neglect any savanna CH_4 flux.

2.3.2 | NEP estimate for the wetland component

Estimates of NEP for the wetland component were based on data from a second OzFlux site, Fogg Dam (AU-Fog; Beringer et al., 2016), a seasonal floodplain ~20 km from the Howard River where CO_2 fluxes were measured for three years from 2006 to 2008 (Beringer et al., 2013). The seasonal wetlands in our target catchment have very similar morphology and vegetation assemblages to those at AU-Fog. In addition, wet and dry season rainfall, temperature, solar radiation and the dynamics of vegetation cover at AU-Fog during the 3 years of observations were comparable to those during our two survey years (Methods S7); hence, we considered that using the average net C flux at AU-Fog as reported by Beringer et al. (2013) as a surrogate to estimate NEP for the wetlands of the Howard River catchment was appropriate. Further details on the representativeness of these asynchronous wetland NEP measurements are provided in the Supporting Information (Methods S7).

2.4 | Quantification of fire-related C emissions

To account for the losses in C through fire across the catchment, we used the SavBAT 2.2 software (Commonwealth of Australia, 2015), an online tool that uses monthly MODIS observations of area burnt and vegetation type to estimate CO_2, CH_4 and N_2O emissions. Based on the premise that fire severity is higher in the late dry season (Russell-Smith & Edwards, 2006), we assigned different patchiness and burning efficiency factors for early (before July 1) versus late (after July 1) dry season fire events. We uploaded shapefiles of the areal extent of each landscape component (i.e. savanna and wetlands) into the SavBAT 2.2 algorithm to derive monthly fire-related CO_2 and CH_4 emissions for each component and for the 2 years of survey (see details in Methods S8 of the Supporting Information). To gain insight into interannual variations, we also quantified annual fire emissions from 2001 to 2018 using SavBAT.

2.5 | Rainfall, runoff and evapotranspiration

Rainfall, runoff and evapotranspiration data were required to derive annual water balances and, in the case of runoff, to convert DIC, DOC and POC concentrations into loads exported. For rainfall, we used four gauges managed by the Bureau of Meteorology (http://bom.gov.au/climate/data) within the catchment (BoM stations 14149, 14192, 14219 and 14226) and derived daily and annual rainfall totals using the mean from the four sites. For runoff, we extracted hourly water discharge measurements for the gauged Howard River (Northern Territory Government station G8150179; https://water.nt.gov.au). Our manual and automated C measurements (DIC, DOC, POC) were undertaken at the gauging station. For evapotranspiration, we divided the latent heat flux data measured at the AU-How flux tower by the temperature-corrected latent heat of vaporization in order to obtain hourly evapotranspiration estimates.

3 | RESULTS

3.1 | Hydrometeorological context

Total rainfall and runoff amounts were similar in both study years (Figure 1a). In year 1, the onset of the monsoon occurred in mid-December and there were 11 major monsoonal events, where events are defined as consecutive rain days with total $P > 100$ mm (the highest event was 400 mm over 8 days). In year 2, the monsoon started later (mid-January) and there were five monsoonal events (the highest event being 710 mm over 7 days). As a result, slightly higher rainfall and runoff totals were recorded in the first year (rainfall 2,400 vs. 2,130 mm and runoff 1,140 vs. 1,050 mm for year 1 and year 2, respectively), but the highest maximum daily discharge occurred in year 2 (83 vs. 144 m^3 s^{-1}; the latter event corresponding to an 8-year return period). Both study years had above average rainfall conditions, the long-term (1989–2018) average being 1,890 mm/year. Both years also had higher annual runoff totals relative to the long-term (1997–2018) average of 680 mm/year.

3.2 | Terrestrial C production

The savanna ecosystem in the Howard River catchment was a strong net C sink during most of the 2-year study period, with an average NEP of 14.4 μg C m^{-2} s^{-1} (Figure 1b). Because GPP generally peaked during the wet season, the sink strength was higher during these periods and comparatively lower in the dry season. There were short periods when the savanna was a weak C source, particularly following the first rainfall events of the early wet season (due to the 'Birch effect' as described by Beringer et al., 2007). Our average annual savanna NEP estimate for AU-How was 455 ± 85 Mg C km^{-2} $year^{-1}$ (Table 1; 524 ± 84 and 380 ± 86 Mg C/km^2 for year 1 and year 2). For the seasonally flooded wetland component, Beringer et al. (2013) reported a higher NEP in the wet season relative to the dry season due to increased plant productivity. We assumed an NEP of 308 ± 19 Mg C km^{-2} $year^{-1}$ (Table 1) derived from the AU-Fog tower site as per Beringer et al. (2013). Note that this estimate does not comprise the offset by CH_4 emissions from wetlands, which was included in the catchment ΣF_{aq} flux (see Section 3.4).

3.3 | Fire-related C emissions

According to our spatially explicit estimates of fire-related CO_2 and CH_4 emissions (F_{fire}), the wetland areas (−62.6 ± 12.5 Mg C km^{-2} $year^{-1}$)
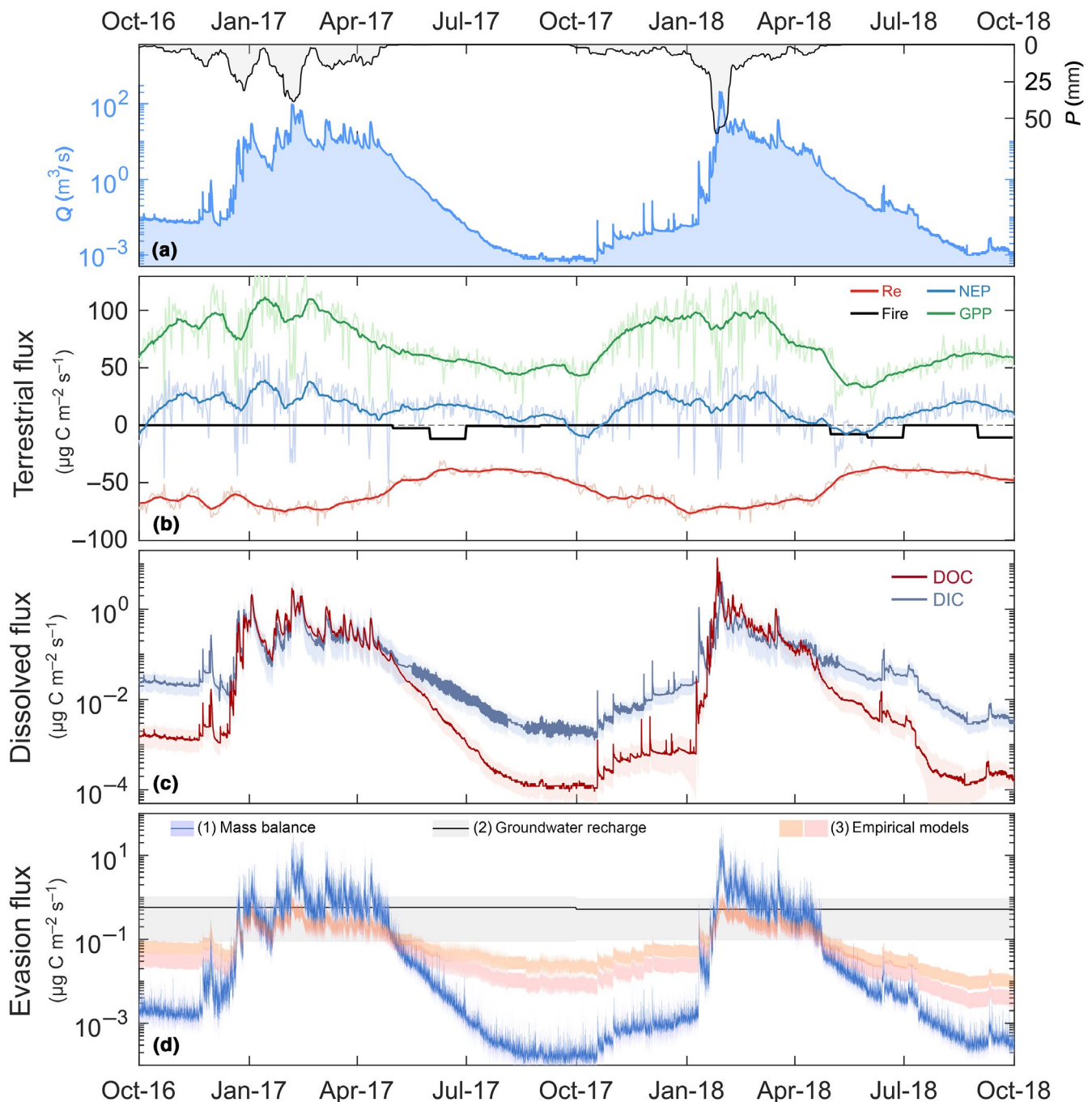
FIGURE 1 Hydrometeorological and C flux data for the Howard River catchment between 2016 and 2018. Time-series of (a) daily precipitation (P, 14-day moving mean) and bi-hourly discharge (Q); (b) daily savanna gross primary production (GPP), respiration (Re) and net ecosystem productivity (NEP) and their 20-day moving means, and monthly fire-related emission flux; (c) bi-hourly DIC and DOC downstream fluxes with lines representing medians and shaded areas representing uncertainties (percentiles 2.5 and 97.5); (d) CO_2 evasion flux according to three methods with lines representing medians and shaded areas representing percentiles 2.5 and 97.5. For empirical models, the inter-percentile ranges are shown only for the lowest (equation 1 in Raymond et al., 2012, red) and highest (equation 2, orange) model outputs for clarity. In (b), positive fluxes indicate a net C sink

were slightly more affected by fire than savanna woodlands (-54.3 ± 10.9 Mg C km^{-2} year^{-1}; Table 1). Using the areal extent of savanna versus seasonal wetland landscape components, we obtained an area-weighted F_{fire} estimate of -56.4 ± 11.3 Mg C km^{-2} year^{-1} for the catchment throughout the study period (Table 1), partitioned into -56.2 Mg CO_2-C km^{-2} year^{-1} and -0.2 Mg CH_4-C km^{-2} year^{-1}

(-40.1 ± 8.0 and -72.6 ± 14.5 Mg C/km^2 for year 1 and year 2), with large monthly variations. Most fires occurred within the first months of the dry season (May–June), except for September 2018 when relatively large areas (~20%) of the savanna and dried grassy floodplains burnt (Figure 1b). The fire emission estimate reported by Beringer et al. (2007) for the flux tower footprint (~-160 Mg C km^{-2} year^{-1})

TABLE 1 Summary of average annual C fluxes in the Howard River catchment for the 1/10/2016–30/9/2018 period. Values in parentheses in the estimate column are values for year 1 and year 2 when available. Uncertainties are expressed as ±2σ unless stated otherwise

Flux	Method	Estimate (Mg C km^{-2} year^{-1})
NEP$_{savanna}$	Eddy covariance	455.2 ± 84.8 (524.0 ± 83.9; 380.4 ± 85.6)
NEP$_{wetland}$	Eddy covariance (Beringer et al., 2013)	308.3 ± 19.2
Area-weighted NEP		**418.6 ± 82.2 (470.3 ± 80.8; 362.4 ± 84.7)**
F$_{fire\ savanna}$[a]	SavBAT 2.2	−54.3 ± 10.9 (−39.2 ± 7.8; −69.4 ± 13.9)
F$_{fire\ wetland}$[a]	SavBAT 2.2	−62.6 ± 12.5 (−42.8 ± 8.6; −82.3 ± 16.5)
Area-weighted F$_{fire}$[a]		**−56.4 ± 11.3 (−40.1 ± 8.0; −72.6 ± 14.5)**
F$_{CH4\ wetland}$	Flux chamber (Beringer et al., 2013)	−4.3 ± 0.6
F$_{DOC}$	High-frequency data	−5.9 ± 0.4 (−5.9 ± 0.4; −6.0 ± 0.8)
F$_{DIC}$	High-frequency data	−4.1 ± 0.2 (−4.6 ± 0.3; −3.5 ± 0.2)
F$_{POC}$	Manual sampling	−1.9 ± 0.7 (−1.7 ± 1.4; −2.0 ± 1.5)
F$_{CO2\ river}$ (method 1)	Mass balance	−12.1 ± 1.4 (−12.3 ± 2.0; −11.4 ± 3.1)
F$_{CO2\ river}$ (method 2)	Groundwater recharge	−17.2 ± 14.4 (−18.0 ± 15.2; −16.3 ± 13.6)
F$_{CO2\ river}$ (method 3)	Model 1	−2.7 ± 0.1 (−3.0 ± 0.1; −2.4 ± 0.1)
	Model 2	−3.5 ± 0.1 (−3.9 ± 0.1; −3.2 ± 0.1)
	Model 7	−3.4 ± 0.1 (−3.8 ± 0.1; −3.1 ± 0.1)
ΣFaq[b]		**−28.2 ± 12.5 (−28.8 ± 24.6; −27.2 ± 22.8)**
NLCB		**334.0 ± 175.3 (401.4 ± 359.4; 262.6 ± 234.5)**

Estimates in bold correspond to totals for each flux.

[a] For these fluxes, the uncertainty was estimated as ±20% of the measured flux.

[b] ΣF$_{aq}$ was calculated based on the CO_2 evasion flux obtained from method 1.

is higher than our catchment-scale estimate, as the latter includes areas of peri-urban development, a land use that features housing on managed native vegetation where fire was largely excluded by owners. Between 2001 and 2018, the fire C emissions varied between −39 and −137 Mg C km^{-2} year^{-1} (average −83 Mg C km^{-2} year^{-1}).

3.4 | Aquatic C fluxes

The POC, DIC and DOC fluxes transported by the river were −1.9 ± 0.7, −4.1 ± 0.2 and −5.9 ± 0.4 Mg C km^{-2} year^{-1}, respectively (Table 1). Because the study period encompassed years of particularly high rainfall, our measured dissolved C fluxes are likely to be in the upper end of the range of possible ΣF$_{aq}$ fluxes for this catchment.

Our estimates of the CO_2 evasion flux (F$_{CO2}$) spanned a wide range depending on the approach used (Figure 1d; Table 1). Estimates based on method 3 (mean −3.2 ± 0.1 Mg C km^{-2} year^{-1} or −3,960 g C m^{-2} year^{-1} of river area) were significantly lower than estimates based on methods 1 and 2 (−12.1 ± 1.4 and −17.2 ± 14.4 Mg C km^{-2} year^{-1} or −14,770 and −20,980 g C m^{-2} year^{-1} of river area; Table 1). Because the pCO$_2$ measurements used in method 3 were taken at the outlet of the catchment, they do not incorporate the higher pCO$_2$ levels measured for middle and upstream reaches (Duvert et al., 2019). As a result, we expect that method 3 will substantially underestimate the true CO_2 evasion flux. While our estimate based on groundwater recharge may be a more reliable

approximation of the evasion flux, this approach suffers from large uncertainties related to the aquifer's specific yield estimation (see Methods S5 in Supporting Information). As such, we considered our mass balance-derived evasion flux (method 1) to be the most realistic estimate.

We also accounted for the flux of CH$_4$ emitted from the seasonal wetlands based on data reported by Beringer et al. (2013). Extrapolating their wet and dry season measurements into an annual estimate, we obtained a flux of −17.2 ± 2.9 g C year^{-1} m^{-2} of wetland area, which once corrected for the surface area occupied by this landscape component (25%) yielded a CH$_4$ contribution of −4.3 ± 0.6 Mg C km^{-2} year^{-1} to the catchment ΣF$_{aq}$ (Table 1). Altogether, the downstream export of DOC, DIC and POC and the F$_{CO2}$ and F$_{CH4}$ evasion fluxes represented an aquatic C export flux of −28.2 ± 12.5 Mg C km^{-2} year^{-1} (Table 1). This flux was relatively similar in years 1 and 2 at −28.8 ± 24.6 and −27.2 ± 22.8 Mg C/km^2, respectively.

3.5 | Net landscape C balance

Using the areal extent of savanna versus seasonal wetland landscape components, we compiled an area-weighted NEP estimate of 418.6 ± 82.2 Mg C km^{-2} year^{-1} for the Howard River catchment. Deducting the aquatic and fire-related losses yields an NLCB of 334.0 ± 175.3 Mg C km^{-2} year^{-1} (Figure 2; 401.4 ± 359.4 and 262.6 ± 234.5 Mg C/km^2 for year 1 and year 2), a significant net C sink in
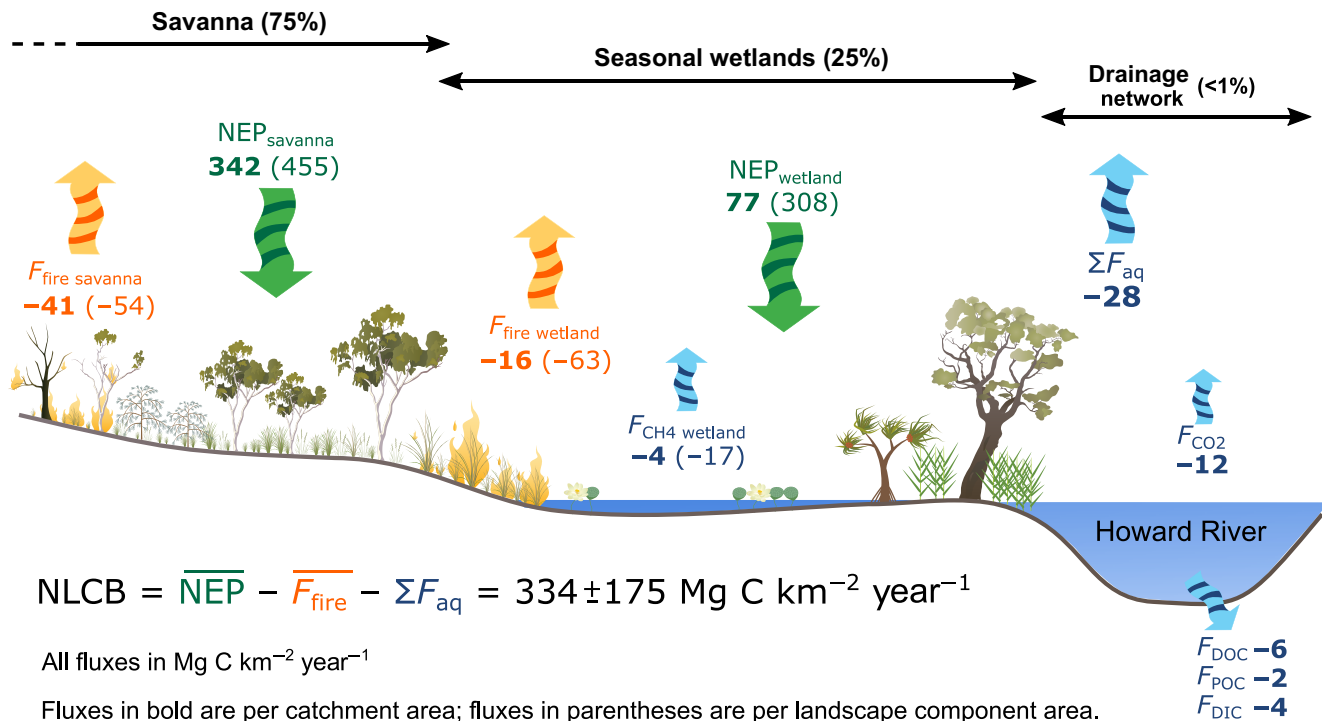
FIGURE 2 Annual net landscape C balance (NLCB) for the Howard River catchment. ΣF_{aq} represents the sum of all aquatic C fluxes, including downstream export (F_{DIC}, F_{DOC}, F_{POC}) and evasion (F_{CO2} and area-weighted F_{CH4} from wetlands). $F_{fire\ savanna}$ and $F_{fire\ wetland}$ correspond to the fire-related C emissions for the savanna and wetland components, respectively, and $\overline{F_{fire}}$ is the area-weighted average for the whole catchment. $NEP_{savanna}$ and $NEP_{wetland}$ are the annual net terrestrial C productivity for the savanna and wetland components, respectively, and $\overline{NEP}$ is the area-weighted average for the whole catchment. Percentages in parentheses for each landscape component at the top of the diagram correspond to area weightings

both years. The aquatic C export and fire-related emissions were found to offset our area-weighted mean NEP by ~7% and ~13%, respectively.

We observed large seasonal variations in NEP, ΣF_{aq} and F_{fire} (Figure 3), with a wet-season peak in NEP that was concomitant with high ΣF_{aq}. Fire was restricted to the dry season, when ΣF_{aq} was <2% of annual fluxes. Assuming that the temporal changes in C storage in the vegetation, soil and freshwater pools were negligible over the 2-year measurement period relative to the observed monthly variations in flux, we examined the seasonal variations in NLCB (black line in Figure 3). Because ΣF_{aq} peaked when NEP was highest, the magnitude of ΣF_{aq} was never large enough to shift the NLCB to a C source. Conversely, high F_{fire} losses occurred when NEP was closer to zero, which led to the catchment becoming a net C exporter during May–June of year 2. We recognize that this temporal analysis is somewhat conceptual, in that the landscape source–sink dynamics could vary further depending on the time-scale of examination. Using daily data, one flooding event that occurred in late January–early February 2018 (year 2) was sufficient to turn the system to a net C source for several days. This single event also accounted for ~39% of annual ΣF_{aq} for year 2.

4 | DISCUSSION

Our landscape-scale approach allowed us to explicitly relate aquatic C export and fire-related emissions to terrestrial C productivity

in a complex catchment of the wet–dry tropics. Our results show that savanna burning can shift the ecosystem to a net C source for several months in the early dry season. Aquatic C exports, despite being of lower magnitude than fire, can also significantly offset NEP during the wet season (by up to 18% for a given month). Here we highlight the uncertainties related to our flux estimates, discuss in more detail the respective roles of aquatic export and fire on the C balance of this landscape, and outline the potential effect of climatic variability on the current and future NLCB of the wet–dry tropical biome.

4.1 | Uncertainties on aquatic C export estimates

Constraining aquatic C fluxes is notoriously difficult, and we recognize a number of limitations to our estimates of ΣF_{aq}. First, recent research has highlighted the inherent difficulty in correctly accounting for riverine CO_2 evasion, because heterogeneities in the surface and subsurface environments make this process highly localized in streams (Duvert, Butman, Marx, Ribolzi, & Hutley, 2018; Lupon et al., 2019; Rocher-Ros, Sponseller, Lidberg, Mörth, & Giesler, 2019). We argue that mass balance methods, as developed in this study, offer a more reliable alternative to more direct assessments of the evasion flux—and not surprisingly, approaches of this kind have been increasingly used in the literature (Davidson et al., 2010; Duvert
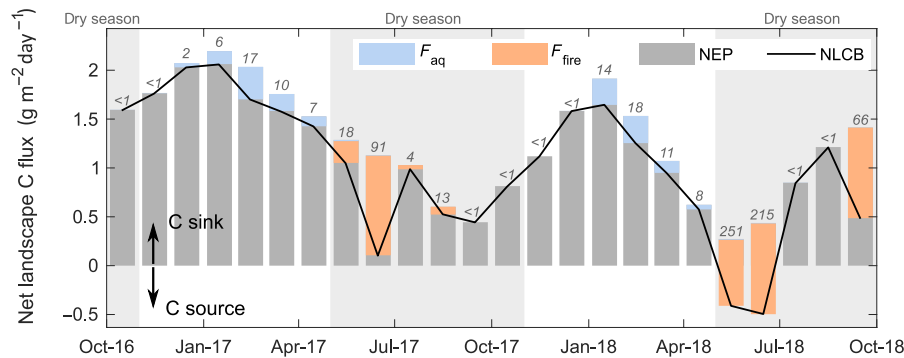
FIGURE 3 Monthly variations in the net landscape C balance (NLCB) of the Howard River catchment between 2016 and 2018. Grey bars represent the monthly net ecosystem productivity (NEP) estimates, while orange and blue bars represent the offset of NEP by fire-related emissions (F_{fire}) and aquatic export (ΣF_{aq}), respectively. The black line represents the net C flux (NLCB) across the 2 years of survey. The numbers in italic at the bottom of each monthly bar correspond to the per cent offset of NEP by the combination of F_{fire} and ΣF_{aq}. Positive NLCB values indicate a net C sink, while negative NLCB values indicate that the ecosystem is shifting to a net C source. ΣF_{aq} was obtained by summing the DIC, DOC, POC, and CO_2 and CH_4 (evasion) fluxes

et al., 2019; Horgby et al., 2019; Hutchins, Tank, et al., 2020). Future efforts should focus on better characterization of the variability of groundwater inputs along rivers, and integrating this flux into catchment and regional C budgets.

Second, several processes are known to modify the pools of dissolved C in rivers. Aquatic metabolism in particular may play an important role in regulating the DIC pool, and while the consumption of CO_2 by microphytes such as algae would be compensated by increased POC flux, the photosynthetic activity of freshwater macrophytes can result in a net uptake of CO_2 or ionic forms of DIC (Iversen et al., 2019). However, low photosynthetic activity can be expected in the often nutrient-limited rivers of the study region (Garcia et al., 2015; Townsend, Webster, & Schult, 2011). The burial of organic matter in the river sediments is another missing term in our C balance, which might be of importance in this lowland river where some sediment deposition occurs in downstream areas. Heterotrophic Re of this organic material stored in the river and riverbed may have added CO_2 and CH_4 to the water column, particularly at the onset of the wet season when the accumulated litter in wetlands and riparian areas is flushed into the river (e.g. Acuña, Giorgi, Muñoz, Sabater, & Sabater, 2007). While any such CO_2 production would have been included in our mass balance, we did not measure the potential flux of CH_4 from the river surface to the atmosphere. We hypothesize that this flux was unlikely to be as high as the CH_4 flux from the wetland component, where the pool of decaying organic material is significantly larger. The relatively limited areal extent of the river network relative to the wetland component (0.4% vs. 24.9% of the catchment area) also suggests that the omission of CH_4 evasion from the river did not result in underestimation of ΣF_{aq}. Stanley et al. (2016) report a fluvial CH_4 flux between 1 and 18 Mg C km^{-2} $year^{-1}$ for tropical savannas and grasslands, which scaled to the Howard River catchment area would yield an efflux of 0.01–0.07 Mg C km^{-2} $year^{-1}$.

Our estimates of CH_4 emissions from wetlands were based on published work in a nearby seasonal wetland (Beringer et al., 2013), but as acknowledged by the authors, the large spatial heterogeneity inherent to CH_4 fluxes would require additional data to better constrain CH_4 emissions across this landscape. Because CH_4 fluxes are often greater in densely vegetated areas, the riparian corridor for instance could contribute higher CH_4 to the atmosphere. Bass et al. (2014) reported higher CH_4 fluxes compared to Beringer et al. (2013) in a similar seasonal floodplain (equivalent to annual emission rates of ~166 Mg C km^{-2} $year^{-1}$). But the data of Bass et al. (2014) were recorded under flooded conditions only, that is, when fluxes were greatest; hence, this value cannot be extrapolated to provide an annual emission rate. In general, more work is needed before we can assess the impact of CH_4 emissions with more confidence. We suggest that future efforts will need to systematically include the ebullitive CH_4 flux, as sensors to measure this potentially important term are becoming available (Maeck, Hofmann, & Lorke, 2014; Maher, Drexl, Tait, Johnston, & Jeffrey, 2019).

In contrast to the potential underestimates of ΣF_{aq} as listed above, there is one aspect of our C budget that may be conducive to an overestimate of F_{CO2}. Some of the terrestrially respired CO_2 may be transferred to wetlands via shallow groundwater flow and be subject to evasion once in that landscape component (Duvert et al., 2020). Because this flux was already integrated in the Re term of the seasonal wetland NEP estimate, we may have accounted twice for this evading CO_2. We chose not to correct for this potential double-accounting as we could not realistically estimate the fraction of wetland-evaded CO_2 of an ultimately terrestrial origin.

4.2 | Relative importance of and controls on fire and aquatic export

Tropical savannas are one of the most frequently burnt ecosystems globally, with large implications for C cycling (Beringer et al., 2007, 2015; Murphy et al., 2019; van der Werf et al., 2010). We found that fire-related emissions had the capacity to reduce or even entirely offset NEP during the dry season (Figure 3). The timing of fire

events was also important, with late dry season fires yielding higher emissions than early dry season fires. There is a long history of research on the effect of fire seasonality in northern Australian savannas, the current understanding being that fires that occur late in the dry season are of greater intensity and extent (Russell-Smith & Edwards, 2006; Williams, Gill, & Moore, 1998), and result in substantially larger greenhouse gas emissions (Russell-Smith et al., 2013, 2017) than early dry season fires. Our analysis also illustrates the importance of fires in the dried floodplain and wetland environments, which generated higher C losses per unit area than upland savannas. Fire is known to significantly affect seasonally flooded tropical wetlands, but the ramifications for C storage are not fully understood (Mitsch et al., 2010). The large interannual variability in fire extent and severity in the Howard River catchment precludes us from providing a credible, long-term magnitude of offset by fire using observations.

Although not as important as fire C losses, aquatic C export also contributed to the reduction of NEP, particularly during the wet season when river flow was greatest (Figure 3). Our ΣF_{aq} estimate of -28.2 Mg C km^{-2} $year^{-1}$ is comparable to values reported elsewhere for the humid tropics (Vihermaa et al., 2016; Waterloo et al., 2006), but lower than the estimate by Shih et al. (2018) who found extremely high DIC loads in a humid, mountainous region. Global averages for downstream C export in tropical rivers were estimated by Huang, Fu, Pan, and Chen (2012) at -2.0, -2.1 and -3.3 Mg C km^{-2} $year^{-1}$ for POC, DOC and DIC loads, respectively. Our load estimates were nearly equivalent (POC) and significantly higher (DOC and DIC) than these global values, a finding that suggests that aquatic C export in the wet–dry tropics may be larger than previously thought, and that more observations are urgently needed in this region. Our DOC load estimate was also higher than that modelled by Birkel et al. (2020) for the same river system (-5.9 vs. -1.9 to -2.3 Mg C km^{-2} $year^{-1}$), which we attribute to the lower (daily) frequency used in the previous modelling work which may have underestimated peak fluxes, and to the inclusion of data from a previous, drier, water-year in the model (Birkel et al., 2020).

Discharge exerted primary control on both DOC and DIC fluxes (Figure 1c), although it is interesting to note the decoupling between DOC and DIC dynamics. While both fluxes peaked at high flow, the DOC flux was 2–10 times higher than the DIC flux during major runoff events. Under baseflow conditions, in contrast, the DIC flux was maintained at a relatively high rate, whereas the DOC flux neared zero. Readers are referred to an extended discussion on concentration–discharge patterns for DIC and DOC in the Supporting Information (Discussion S1).

Despite the significance of downstream DOC and DIC loads, CO_2 evasion was identified as the largest contribution to ΣF_{aq} by far, consistent with Duvert et al. (2020) and similar to recent work in tropical landscapes dominated by wetlands (Borges et al., 2019; Hastie et al., 2019). Altogether, our estimates of ΣF_{aq} have the potential to offset estimates of the annual terrestrial C sink by about 7%—an offset that could be potentially much higher in less productive areas of the wet–dry tropics (see Section 4.3).

4.3 | Towards an NLCB for the wet–dry tropical biome

Given the global land area occupied by seasonal tropical ecosystems, developing credible NLCB estimates for the wet–dry tropics is critical to both constraining the global C cycle and predicting impacts of enhanced climatic variability. Few studies have simultaneously captured a time-series of NEP and aquatic C export in the tropical savanna biome (although our wetland NEP estimate was derived from asynchronous measurements). Several studies have focused on the less seasonal Amazon basin, but very few have accounted for all the terms making up ΣF_{aq}, with only one accounting for both ΣF_{aq} and F_{fire} (Hastie et al., 2019). Waterloo et al. (2006) only considered DOC and POC export, Davidson et al. (2010) only considered CO_2 evasion and Zhou et al. (2013) did not account for CO_2 evasion. All these studies yielded a relatively low reduction of the NEP sink strength by ΣF_{aq} (5%–6%, 2%–3% and 3%, respectively). However, a different pattern is now emerging from more complete assessments of ΣF_{aq} and of its role in offsetting NEP. In a small catchment of the Amazon, Vihermaa et al. (2016) found that combining all terms of ΣF_{aq} could reduce NEP by 43%–60%. At the scale of the entire Amazon basin, new modelling by Hastie et al. (2019) suggests that 78% of NEP was lost via aquatic flux, mostly through CO_2 evasion from wetlands and floodplains. When including the effects of fire and harvest, the offset even reached 96% (Hastie et al., 2019). In the Congo River basin, Borges et al. (2019) compared their estimates of CO_2 evasion to an approximation of the terrestrial NEP for the region, and concluded that losses via ΣF_{aq} were three times larger than NEP. They reasoned that only an additional C source from the extensive wetlands (flooded gallery forests), not accounted for in terrestrial NEP estimates, could explain such a disproportionately large ΣF_{aq} term.

Our estimate of the per cent loss of NEP by ΣF_{aq}, arguably the first for the wet–dry tropics, is relatively small (~7%) compared to the recent studies described above, and significantly lower than our estimate of the NEP offset by fire. Nevertheless, our conclusion that the offset by ΣF_{aq} is small relative to NEP may not hold for other areas of the wet–dry tropical biome. The Howard River catchment is located in a high rainfall, coastal savanna area that represents a relatively small proportion (~60,000 km^2) of the total extent of tropical savannas in Australia (1.92 million km^2; Hutley et al., 2011), where wetlands may occupy a larger proportion of the landscape than in drier areas of the wet–dry tropics and where NEP is at the upper end of the global average for this biome (Beringer et al., 2007; Chen et al., 2003; Grace, José, Meir, Miranda, & Montes, 2006). The high NEP observed at AU-How can be attributed to a range of factors. Hutley and Beringer (2011) demonstrated that despite frequent fire, the site is experiencing vegetation thickening post-Cyclone Tracy (1974), with a tree sink of ~50 Mg C km^{-2} $year^{-1}$. This tree sink may well be underestimated due to incomplete biomass inventory when using allometric methods (Calders et al., 2015; Gonzalez de Tanago et al., 2018), as was undertaken here. Accumulation of soil C may also be occurring at

the site, although previous studies on changes in soil C stock in tropical savannas have been inconclusive (Allen et al., 2014). Lastly, charcoal production can be another significant sink in fire-prone landscapes (Jones, Santín, van der Werf, & Doerr, 2019), and is known to represent about 10% of biomass burnt in Australian tropical savannas (Saiz et al., 2015).

Areas to the south of the Howard River that receive lower rainfall are much weaker C sinks (Beringer et al., 2015), and so ΣF_{aq} could affect NEP more significantly in these areas, in line with Webb et al. (2019) who found that the relative importance of ΣF_{aq} increased with decreasing NEP. For instance, the Litchfield savanna supersite, located 85 km southwest of Howard Springs (Karan et al., 2016), had an average NEP of 82 Mg C km^{-2} year^{-1} for the two water-years corresponding to our survey (J. Beringer & L. B. Hutley, 2020, unpublished data). This is less than a fifth of NEP at the Howard River catchment, for similar annual rainfall (~1,900 mm)—although this site experiences frequent high-severity fires and has a biomass 30% lower than AU-How. While it is difficult to scale our estimates of ΣF_{aq} to the Litchfield area, given the role of runoff in controlling ΣF_{aq} it would be reasonable to assume the aquatic C flux to be of similar magnitude to that measured for the Howard River, and so the offset would reach ~30%–35% of NEP in that case. We postulate that the reduction of NEP by ΣF_{aq} might be even more disproportionate in areas of the wet–dry tropics where the strength of the terrestrial sink is even weaker. Clearly, more studies are needed to upscale this first NLCB estimate to less productive, yet hydrologically dynamic regions of the wet–dry tropics.

Even though ΣF_{aq} was found to be less important in this tropical savanna landscape than in wetter regions of the tropics, it is an important flux to consider if we are to develop credible NLCBs. This is particularly critical in tropical ecosystems, which unlike our study site are often weak C sinks (Beringer et al., 2015; Vihermaa et al., 2016). In these pulse-driven landscapes more than anywhere else, high-frequency surveys of ΣF_{aq} are essential, as we showed that a single flooding event (e.g. the January–February event in 2018) could account for 39% of annual ΣF_{aq}.

4.4 | Feedbacks between NLCB and current and future climate

Climatic conditions are known to exert a strong control on both terrestrial C production (NEP) and export (ΣF_{aq} and F_{fire}; Hastie et al., 2019; Öquist et al., 2014; Song et al., 2020; Webb et al., 2019). While we were not able to test the relationship between annual rainfall and ΣF_{aq} because of the limited number of years of observations, significant connections between rainfall and ΣF_{aq} have been reported in many parts of the world including the tropics (Butman et al., 2016; Chi et al., 2020; Hastie et al., 2019; Öquist et al., 2014; Rasera, Krusche, Richey, Ballester, & Victória, 2013). It would be reasonable to expect the same pattern in the Howard River, that is, wet years fuelling aquatic C export, because of the high sensitivity of ΣF_{aq} to discharge (Figure 1c,d). Given the relatively predictable

behaviour of dissolved and evasion fluxes, and provided robust calibration with additional years of data, we envisage that in the future ΣF_{aq} can be predicted using discharge data.

More complex is the relationship between rainfall and NEP, particularly in the tropics (Baldocchi, Chu, & Reichstein, 2018) where wetter years were associated with either a greater (Zeri et al., 2014) or a smaller (Yan et al., 2013) terrestrial C sink. In the Howard River catchment, wetter conditions may result in increased grass production, but other controlling factors such as light limitations from persistent cloud cover during the wet season have been found to complicate the response of NEP to changes in rainfall (Whitley et al., 2011).

Climate change will bring longer and more intense heatwaves in northern Australia (Herold et al., 2018). Models also suggest a 5%–20% increase in monsoon rainfall over the second half of the 20th century (Jourdain et al., 2013), although uncertainties remain on the effect of climate change on rainfall in tropical Australia (Dey, Lewis, Arblaster, & Abram, 2019). These potential changes will have important yet unknown ramifications on the NLCB of the wet–dry tropics. Hastie et al. (2019) showed that annual increases in the terrestrial C sink in the Amazon basin were offset by greater C losses via ΣF_{aq}. Likewise, we hypothesize that increased atmospheric CO_2, wetter conditions and more intense events in northern Australia will together increase wet-season terrestrial C production but also aquatic C export. Combined with hotter conditions in the dry season, these scenarios may also lead to an increase in fire C emissions, potentially further offsetting the current C sink. However, integrating fire emissions to NLCB predictions is difficult as savanna burning is typically driven by a combination of biophysical and societal factors (Russell-Smith et al., 2013).

The tropical savanna NLCB may shift from a weak C sink to a C source in the future due to hotter and wetter climate and the combined effect of increased fire and aquatic export. To better predict and mitigate future changes in the tropical savanna NLCB, we need more integrative views of C cycling between the different landscape components and aquatic systems, and a better understanding of the long-term feedbacks between climate, NEP, fire and aquatic C export (Chi et al., 2020; Hastie et al., 2019).

ORCID

Clément Duvert (iD) https://orcid.org/0000-0002-9873-6846
Lindsay B. Hutley (iD) https://orcid.org/0000-0001-5533-9886
Jason Beringer (iD) https://orcid.org/0000-0002-4619-8361
Michael I. Bird (iD) https://orcid.org/0000-0003-1801-8703
Christian Birkel (iD) https://orcid.org/0000-0002-6792-852X
Damien T. Maher (iD) https://orcid.org/0000-0003-1899-005X
Mitchel Rudge (iD) https://orcid.org/0000-0003-2079-7195
Samantha A. Setterfield (iD) https://orcid.org/0000-0002-7470-4997
Jonathan G. Wynn (iD) https://orcid.org/0000-0001-8118-024X

REFERENCES

Abril, G., & Borges, A. V. (2019). Ideas and perspectives: Carbon leaks from flooded land: Do we need to replumb the inland water active pipe? *Biogeosciences*, 16(3), 769–784. https://doi.org/10.5194/bg-16-769-2019

Abril, G., Martinez, J.-M., Artigas, L. F., Moreira-Turcq, P., Benedetti, M. F., Vidal, L., ... Roland, F. (2014). Amazon River carbon dioxide outgassing fuelled by wetlands. *Nature*, 505, 395–398. https://doi.org/10.1038/nature12797

Acuña, V., Giorgi, A., Muñoz, I., Sabater, F., & Sabater, S. (2007). Meteorological and riparian influences on organic matter dynamics in a forested Mediterranean stream. *Journal of the North American Benthological Society*, 26(1), 54–69. https://doi.org/10.1899/0887-3593(2007)26[54:Marioo]2.0.Co;2

Allen, D. E., Bloesch, P. M., Cowley, R. A., Orton, T. G., Payne, J. E., & Dalal, R. C. (2014). Impacts of fire on soil organic carbon stocks in a grazed semi-arid tropical Australian savanna: Accounting for landscape variability. *The Rangeland Journal*, 36(4), 359–369. https://doi.org/10.1071/RJ14044

Aufdenkampe, A. K., Mayorga, E., Raymond, P. A., Melack, J. M., Doney, S. C., Alin, S. R., ... Yoo, K. (2011). Riverine coupling of biogeochemical cycles between land, oceans, and atmosphere. *Frontiers in Ecology and the Environment*, 9(1), 53–60. https://doi.org/10.1890/100014

Baldocchi, D., Chu, H., & Reichstein, M. (2018). Inter-annual variability of net and gross ecosystem carbon fluxes: A review. *Agricultural and Forest Meteorology*, 249, 520–533. https://doi.org/10.1016/j.agrformet.2017.05.015

Bass, A. M., Bird, M. I., Munksgaard, N. C., & Wurster, C. M. (2012). ISO-CADICA: Isotopic – Continuous, automated dissolved inorganic carbon analyser. *Rapid Communications in Mass Spectrometry*, 26(6), 639–644. https://doi.org/10.1002/rcm.6143

Bass, A. M., O'Grady, D., Leblanc, M., Tweed, S., Nelson, P. N., & Bird, M. I. (2014). Carbon dioxide and methane emissions from a wet-dry tropical floodplain in Northern Australia. *Wetlands*, 34(3), 619–627. https://doi.org/10.1007/s13157-014-0522-5

Beck, H. E., Zimmermann, N. E., McVicar, T. R., Vergopolan, N., Berg, A., & Wood, E. F. (2018). Present and future Köppen-Geiger climate classification maps at 1-km resolution. *Scientific Data*, 5(1), 180214. https://doi.org/10.1038/sdata.2018.214

Beringer, J., Hutley, L. B., Abramson, D., Arndt, S. K., Briggs, P., Bristow, M., ... Uotila, P. (2015). Fire in Australian savannas: From leaf to landscape. *Global Change Biology*, 21(1), 62–81. https://doi.org/10.1111/gcb.12686

Beringer, J., Hutley, L. B., McHugh, I., Arndt, S. K., Campbell, D., Cleugh, H. A., ... Wardlaw, T. (2016). An introduction to the Australian and New Zealand flux tower network – OzFlux. *Biogeosciences*, 13(21), 5895–5916. https://doi.org/10.5194/bg-13-5895-2016

Beringer, J., Hutley, L. B., Tapper, N. J., & Cernusak, L. A. (2007). Savanna fires and their impact on net ecosystem productivity in North Australia. *Global Change Biology*, 13(5), 990–1004. https://doi.org/10.1111/j.1365-2486.2007.01334.x

Beringer, J., Livesley, S. J., Randle, J., & Hutley, L. B. (2013). Carbon dioxide fluxes dominate the greenhouse gas exchanges of a seasonal wetland in the wet–dry tropics of northern Australia. *Agricultural and Forest Meteorology*, 182–183, 239–247. https://doi.org/10.1016/j.agrformet.2013.06.008

Beringer, J., McHugh, I., Hutley, L. B., Isaac, P., & Kljun, N. (2017). Technical note: Dynamic INtegrated Gap-filling and partitioning for OzFlux (DINGO). *Biogeosciences*, 14(6), 1457–1460. https://doi.org/10.5194/bg-14-1457-2017

Billett, M. F., Palmer, S. M., Hope, D., Deacon, C., Storeton-West, R., Hargreaves, K. J., ... Fowler, D. (2004). Linking land-atmosphere-stream carbon fluxes in a lowland peatland system. *Global Biogeochemical Cycles*, 18(1). https://doi.org/10.1029/2003gb002058

Birkel, C., Duvert, C., Correa, A., Munksgaard, N. C., Maher, D. T., & Hutley, L. B. (2020). Tracer-aided modelling in the low-relief, wet-dry tropics suggests water ages and DOC export are driven by seasonal wetlands and deep groundwater. *Water Resources Research*, 56(4), e2019WR026175. https://doi.org/10.1029/2019WR026175

Borges, A. V., Darchambeau, F., Lambert, T., Morana, C., Allen, G. H., Tambwe, E., ... Bouillon, S. (2019). Variations in dissolved greenhouse gases (CO_2, CH_4, N_2O) in the Congo River network overwhelmingly driven by fluvial-wetland connectivity. *Biogeosciences*, 16(19), 3801–3834. https://doi.org/10.5194/bg-16-3801-2019

Borges, A. V., Darchambeau, F., Teodoru, C. R., Marwick, T. R., Tamooh, F., Geeraert, N., ... Bouillon, S. (2015). Globally significant greenhouse-gas emissions from African inland waters. *Nature Geoscience*, 8, 637–642. https://doi.org/10.1038/ngeo2486

Butman, D., Stackpoole, S., Stets, E., McDonald, C. P., Clow, D. W., & Striegl, R. G. (2016). Aquatic carbon cycling in the conterminous United States and implications for terrestrial carbon accounting. *Proceedings of the National Academy of Sciences of the United States of America*, 113(1), 58–63. https://doi.org/10.1073/pnas.1512651112

Calders, K., Newnham, G., Burt, A., Murphy, S., Raumonen, P., Herold, M., ... Kaasalainen, M. (2015). Nondestructive estimates of aboveground biomass using terrestrial laser scanning. *Methods in Ecology and Evolution*, 6(2), 198–208. https://doi.org/10.1111/2041-210x.12301

Chapin, F. S., Woodwell, G. M., Randerson, J. T., Rastetter, E. B., Lovett, G. M., Baldocchi, D. D., ... Schulze, E.-D. (2006). Reconciling carbon-cycle concepts, terminology, and methods. *Ecosystems*, 9(7), 1041–1050. https://doi.org/10.1007/s10021-005-0105-7

Chen, X., Hutley, L. B., & Eamus, D. (2003). Carbon balance of a tropical savanna of northern Australia. *Oecologia*, 137(3), 405–416. https://doi.org/10.1007/s00442-003-1358-5

Chi, J., Nilsson, M. B., Laudon, H., Lindroth, A., Wallerman, J., Fransson, J. E. S., … Peichl, M. (2020). The Net Landscape Carbon Balance – Integrating terrestrial and aquatic carbon fluxes in a managed boreal forest landscape in Sweden. *Global Change Biology*, *26*(4), 2353–2367. https://doi.org/10.1111/gcb.14983

Chuvieco, E. (2009). Global impacts of fire. In E. Chuvieco (Ed.), *Earth observation of wildland fires in Mediterranean ecosystems* (pp. 1–10). Berlin, Heidelberg: Springer.

Commonwealth of Australia. (2015). *Carbon credits (carbon farming initiative – Emissions abatement through savanna fire management) methodology determination 2015*. Canberra, Australia: ComLaw. Retrieved from http://www.comlaw.gov.au/Details/F2015L00344

Cook, P. G., Hatton, T. J., Pidsley, D., Herczeg, A. L., Held, A., O'Grady, A., & Eamus, D. (1998). Water balance of a tropical woodland ecosystem, Northern Australia: A combination of micro-meteorological, soil physical and groundwater chemical approaches. *Journal of Hydrology*, *210*(1), 161–177. https://doi.org/10.1016/S0022-1694(98)00181-4

Davidson, E. A., Figueiredo, R. O., Markewitz, D., & Aufdenkampe, A. K. (2010). Dissolved CO_2 in small catchment streams of eastern Amazonia: A minor pathway of terrestrial carbon loss. *Journal of Geophysical Research: Biogeosciences*, *115*(G4), G04005. https://doi.org/10.1029/2009JG001202

Dey, R., Lewis, S. C., Arblaster, J. M., & Abram, N. J. (2019). A review of past and projected changes in Australia's rainfall. *Wiley Interdisciplinary Reviews: Climate Change*, *10*(3), e577. https://doi.org/10.1002/wcc.577

Drake, T. W., Raymond, P. A., & Spencer, R. G. M. (2018). Terrestrial carbon inputs to inland waters: A current synthesis of estimates and uncertainty. *Limnology and Oceanography Letters*, *3*(3), 132–142. https://doi.org/10.1002/lol2.10055

Duvert, C., Bossa, M., Tyler, K. J., Wynn, J. G., Munksgaard, N. C., Bird, M. I., … Hutley, L. B. (2019). Groundwater-derived DIC and carbonate buffering enhance fluvial CO_2 evasion in two Australian tropical rivers. *Journal of Geophysical Research: Biogeosciences*, *124*(2), 312–327. https://doi.org/10.1029/2018jg004912

Duvert, C., Butman, D. E., Marx, A., Ribolzi, O., & Hutley, L. B. (2018). CO_2 evasion along streams driven by groundwater inputs and geomorphic controls. *Nature Geoscience*, *11*(11), 813–818. https://doi.org/10.1038/s41561-018-0245-y

Duvert, C., Hutley, L. B., Birkel, C., Rudge, M., Munksgaard, N. C., Wynn, J. G., … Bird, M. I. (2020). Seasonal shift from biogenic to geogenic fluvial carbon caused by changing water sources in the wet-dry tropics. *Journal of Geophysical Research: Biogeosciences*, *125*, e2019JG005384. https://doi.org/10.1029/2019JG005384

Friedlingstein, P., Jones, M. W., O'Sullivan, M., Andrew, R. M., Hauck, J., Peters, G. P., … Zaehle, S. (2019). Global carbon budget 2019. *Earth System Science Data*, *11*(4), 1783–1838. https://doi.org/10.5194/essd-11-1783-2019

Garcia, E. A., Pettit, N. E., Warfe, D. M., Davies, P. M., Kyne, P. M., Novak, P., & Douglas, M. M. (2015). Temporal variation in benthic primary production in streams of the Australian wet–dry tropics. *Hydrobiologia*, *760*(1), 43–55. https://doi.org/10.1007/s10750-015-2301-6

Gonzalez de Tanago, J., Lau, A., Bartholomeus, H., Herold, M., Avitabile, V., Raumonen, P., … Calders, K. (2018). Estimation of above-ground biomass of large tropical trees with terrestrial LiDAR. *Methods in Ecology and Evolution*, *9*(2), 223–234. https://doi.org/10.1111/2041-210x.12904

Grace, J., José, J. S., Meir, P., Miranda, H. S., & Montes, R. A. (2006). Productivity and carbon fluxes of tropical savannas. *Journal of Biogeography*, *33*(3), 387–400. https://doi.org/10.1111/j.1365-2699.2005.01448.x

Harned, H. S., & Davis, R. (1943). The ionization constant of carbonic acid in water and the solubility of carbon dioxide in water and aqueous salt solutions from 0 to 50°. *Journal of the American Chemical Society*, *65*(10), 2030–2037. https://doi.org/10.1021/ja01250a059

Hastie, A., Lauerwald, R., Ciais, P., & Regnier, P. (2019). Aquatic carbon fluxes dampen the overall variation of net ecosystem productivity in the Amazon basin: An analysis of the interannual variability in the boundless carbon cycle. *Global Change Biology*, *25*(6), 2094–2111. https://doi.org/10.1111/gcb.14620

Haverd, V., Raupach, M. R., Briggs, P. R., Davis, S. J., Law, R. M., Meyer, C. P., … Sherman, B. (2013). The Australian terrestrial carbon budget. *Biogeosciences*, *10*(2), 851–869. https://doi.org/10.5194/bg-10-851-2013

Healy, R. W., & Cook, P. G. (2002). Using groundwater levels to estimate recharge. *Hydrogeology Journal*, *10*(1), 91–109. https://doi.org/10.1007/s10040-001-0178-0

Herold, N., Ekström, M., Kala, J., Goldie, J., & Evans, J. P. (2018). Australian climate extremes in the 21st century according to a regional climate model ensemble: Implications for health and agriculture. *Weather and Climate Extremes*, *20*, 54–68. https://doi.org/10.1016/j.wace.2018.01.001

Horgby, Å., Segatto, P. L., Bertuzzo, E., Lauerwald, R., Lehner, B., Ulseth, A. J., … Battin, T. J. (2019). Unexpected large evasion fluxes of carbon dioxide from turbulent streams draining the world's mountains. *Nature Communications*, *10*(1), 4888. https://doi.org/10.1038/s41467-019-12905-z

Huang, T.-H., Fu, Y.-H., Pan, P.-Y., & Chen, C.-T.-A. (2012). Fluvial carbon fluxes in tropical rivers. *Current Opinion in Environmental Sustainability*, *4*(2), 162–169. https://doi.org/10.1016/j.cosust.2012.02.004

Hutchins, R. H. S., Casas-Ruiz, J. P., Prairie, Y. T., & del Giorgio, P. A. (2020). Magnitude and drivers of integrated fluvial network greenhouse gas emissions across the boreal landscape in Québec. *Water Research*, *173*, 115556. https://doi.org/10.1016/j.watres.2020.115556

Hutchins, R. H. S., Tank, S. E., Olefeldt, D., Quinton, W. L., Spence, C., Dion, N., … Mengistu, S. G. (2020). Fluvial CO_2 and CH_4 patterns across wildfire-disturbed ecozones of subarctic Canada: Current status and implications for future change. *Global Change Biology*, *26*(4), 2304–2319. https://doi.org/10.1111/gcb.14960

Hutley, L., & Beringer, J. (2011). Disturbance and climatic drivers of carbon dynamics of a north Australian tropical savanna. In M. Hill & N. Hanan (Eds.), *Ecosystem function in savannas: Measurement and modeling at landscape to global scales* (pp. 57–75). Boca Raton, FL: CRC Press.

Hutley, L. B., Beringer, J., Isaac, P. R., Hacker, J. M., & Cernusak, L. A. (2011). A sub-continental scale living laboratory: Spatial patterns of savanna vegetation over a rainfall gradient in northern Australia. *Agricultural and Forest Meteorology*, *151*(11), 1417–1428. https://doi.org/10.1016/j.agrformet.2011.03.002

Isaac, P., Cleverly, J., McHugh, I., van Gorsel, E., Ewenz, C., & Beringer, J. (2017). OzFlux data: Network integration from collection to curation. *Biogeosciences*, *14*(12), 2903–2928. https://doi.org/10.5194/bg-14-2903-2017

Iversen, L. L., Winkel, A., Baastrup-Spohr, L., Hinke, A. B., Alahuhta, J., Baattrup-Pedersen, A., … Pedersen, O. (2019). Catchment properties and the photosynthetic trait composition of freshwater plant communities. *Science*, *366*(6467), 878–881. https://doi.org/10.1126/science.aay5945

Jones, M. W., Santín, C., van der Werf, G. R., & Doerr, S. H. (2019). Global fire emissions buffered by the production of pyrogenic carbon. *Nature Geoscience*, *12*(9), 742–747. https://doi.org/10.1038/s41561-019-0403-x

Jourdain, N. C., Gupta, A. S., Taschetto, A. S., Ummenhofer, C. C., Moise, A. F., & Ashok, K. (2013). The Indo-Australian monsoon and its relationship to ENSO and IOD in reanalysis data and the CMIP3/CMIP5 simulations. *Climate Dynamics*, *41*(11), 3073–3102. https://doi.org/10.1007/s00382-013-1676-1

Karan, M., Liddell, M., Prober, S. M., Arndt, S., Beringer, J., Boer, M., … Wardlaw, T. (2016). The Australian SuperSite Network: A continental, long-term terrestrial ecosystem observatory. *Science of the Total Environment*, *568*, 1263–1274. https://doi.org/10.1016/j.scitotenv.2016.05.170

Kirschbaum, M. U. F., Zeng, G., Ximenes, F., Giltrap, D. L., & Zeldis, J. R. (2019). Towards a more complete quantification of the global carbon cycle. *Biogeosciences*, 16(3), 831–846. https://doi.org/10.5194/bg-16-831-2019

Kling, G. W., Kipphut, G. W., & Miller, M. C. (1991). Arctic lakes and streams as gas conduits to the atmosphere: Implications for tundra carbon budgets. *Science*, 251(4991), 298–301. https://doi.org/10.1126/science.251.4991.298

Lauerwald, R., Laruelle, G. G., Hartmann, J., Ciais, P., & Regnier, P. A. G. (2015). Spatial patterns in CO_2 evasion from the global river network. *Global Biogeochemical Cycles*, 29(5), 534–554. https://doi.org/10.1002/2014GB004941

Livesley, S. J., Grover, S., Hutley, L. B., Jamali, H., Butterbach-Bahl, K., Fest, B., … Arndt, S. K. (2011). Seasonal variation and fire effects on CH_4, N_2O and CO_2 exchange in savanna soils of northern Australia. *Agricultural and Forest Meteorology*, 151(11), 1440–1452. https://doi.org/10.1016/j.agrformet.2011.02.001

Lupon, A., Denfeld, B. A., Laudon, H., Leach, J., Karlsson, J., & Sponseller, R. A. (2019). Groundwater inflows control patterns and sources of greenhouse gas emissions from streams. *Limnology and Oceanography*, 64(4), 1545–1557. https://doi.org/10.1002/lno.11134

Maeck, A., Hofmann, H., & Lorke, A. (2014). Pumping methane out of aquatic sediments – Ebullition forcing mechanisms in an impounded river. *Biogeosciences*, 11(11), 2925–2938. https://doi.org/10.5194/bg-11-2925-2014

Maher, D. T., Drexl, M., Tait, D. R., Johnston, S. G., & Jeffrey, L. C. (2019). iAMES: An inexpensive, automated methane ebullition sensor. *Environmental Science & Technology*, 53(11), 6420–6426. https://doi.org/10.1021/acs.est.9b01881

Mitsch, W. J., Nahlik, A., Wolski, P., Bernal, B., Zhang, L., & Ramberg, L. (2010). Tropical wetlands: Seasonal hydrologic pulsing, carbon sequestration, and methane emissions. *Wetlands Ecology and Management*, 18(5), 573–586. https://doi.org/10.1007/s11273-009-9164-4

Moore, C. E., Beringer, J., Donohue, R. J., Evans, B., Exbrayat, J.-F., Hutley, L. B., & Tapper, N. J. (2018). Seasonal, interannual and decadal drivers of tree and grass productivity in an Australian tropical savanna. *Global Change Biology*, 24(6), 2530–2544. https://doi.org/10.1111/gcb.14072

Murphy, B. P., Prior, L. D., Cochrane, M. A., Williamson, G. J., & Bowman, D. M. J. S. (2019). Biomass consumption by surface fires across Earth's most fire prone continent. *Global Change Biology*, 25(1), 254–268. https://doi.org/10.1111/gcb.14460

Öquist, M. G., Bishop, K., Grelle, A., Klemedtsson, L., Köhler, S. J., Laudon, H., … Nilsson, M. B. (2014). The full annual carbon balance of boreal forests is highly sensitive to precipitation. *Environmental Science & Technology Letters*, 1(7), 315–319. https://doi.org/10.1021/ez500169j

Plummer, L. N., & Busenberg, E. (1982). The solubilities of calcite, aragonite and vaterite in CO_2-H_2O solutions between 0 and 90°C, and an evaluation of the aqueous model for the system $CaCO_3$-CO_2-H_2O. *Geochimica et Cosmochimica Acta*, 46(6), 1011–1040. https://doi.org/10.1016/0016-7037(82)90056-4

Rasera, M. D. F. F. L., Krusche, A. V., Richey, J. E., Ballester, M. V. R., & Victória, R. L. (2013). Spatial and temporal variability of pCO_2 and CO_2 efflux in seven Amazonian Rivers. *Biogeochemistry*, 116(1), 241–259. https://doi.org/10.1007/s10533-013-9854-0

Raymond, P. A., Hartmann, J., Lauerwald, R., Sobek, S., McDonald, C., Hoover, M., … Guth, P. (2013). Global carbon dioxide emissions from inland waters. *Nature*, 503(7476), 355–359. https://doi.org/10.1038/nature12760

Raymond, P. A., Zappa, C. J., Butman, D., Bott, T. L., Potter, J., Mulholland, P., … Newbold, D. (2012). Scaling the gas transfer velocity and hydraulic geometry in streams and small rivers. *Limnology and Oceanography: Fluids and Environments*, 2(1), 41–53. https://doi.org/10.1215/21573689-1597669

Regnier, P., Friedlingstein, P., Ciais, P., Mackenzie, F. T., Gruber, N., Janssens, I. A., … Thullner, M. (2013). Anthropogenic perturbation of the carbon fluxes from land to ocean. *Nature Geoscience*, 6(8), 597–607. https://doi.org/10.1038/ngeo1830

Rocher-Ros, G., Sponseller, R. A., Lidberg, W., Mörth, C.-M., & Giesler, R. (2019). Landscape process domains drive patterns of CO_2 evasion from river networks. *Limnology and Oceanography Letters*, 4(4), 87–95. https://doi.org/10.1002/lol2.10108

Runkel, R. L., Crawford, C. G., & Cohn, T. A. (2004). *Load estimator (LOADEST): A FORTRAN program for estimating constituent loads in streams and rivers (4–A5)*. Retrieved from http://pubs.er.usgs.gov/publication/tm4A5

Russell-Smith, J., Cook, G. D., Cooke, P. M., Edwards, A. C., Lendrum, M., Meyer, C., & Whitehead, P. J. (2013). Managing fire regimes in north Australian savannas: Applying Aboriginal approaches to contemporary global problems. *Frontiers in Ecology and the Environment*, 11(s1), e55–e63. https://doi.org/10.1890/120251

Russell-Smith, J., & Edwards, A. C. (2006). Seasonality and fire severity in savanna landscapes of monsoonal northern Australia. *International Journal of Wildland Fire*, 15(4), 541–550. https://doi.org/10.1071/WF05111

Russell-Smith, J., Monagle, C., Jacobsohn, M., Beatty, R. L., Bilbao, B., Millán, A., … Sánchez-Rose, I. (2017). Can savanna burning projects deliver measurable greenhouse emissions reductions and sustainable livelihood opportunities in fire-prone settings? *Climatic Change*, 140(1), 47–61. https://doi.org/10.1007/s10584-013-0910-5

Saiz, G., Wynn, J. G., Wurster, C. M., Goodrick, I., Nelson, P. N., & Bird, M. I. (2015). Pyrogenic carbon from tropical savanna burning: Production and stable isotope composition. *Biogeosciences*, 12(6), 1849–1863. https://doi.org/10.5194/bg-12-1849-2015

Santos, I. R., Maher, D. T., & Eyre, B. D. (2012). Coupling automated radon and carbon dioxide measurements in coastal waters. *Environmental Science & Technology*, 46(14), 7685–7691. https://doi.org/10.1021/es301961b

Shih, Y.-T., Chen, P.-H., Lee, L.-C., Liao, C.-S., Jien, S.-H., Shiah, F.-K., … Huang, J.-C. (2018). Dynamic responses of DOC and DIC transport to different flow regimes in a subtropical small mountainous river. *Hydrology and Earth System Sciences*, 22(12), 6579–6590. https://doi.org/10.5194/hess-22-6579-2018

Song, C., Wang, G., Hu, Z., Zhang, T., Huang, K., Chen, X., & Li, Y. (2020). Net ecosystem carbon budget of a grassland ecosystem in central Qinghai-Tibet Plateau: Integrating terrestrial and aquatic carbon fluxes at catchment scale. *Agricultural and Forest Meteorology*, 290, 108021. https://doi.org/10.1016/j.agrformet.2020.108021

Stanley, E. H., Casson, N. J., Christel, S. T., Crawford, J. T., Loken, L. C., & Oliver, S. K. (2016). The ecology of methane in streams and rivers: Patterns, controls, and global significance. *Ecological Monographs*, 86(2), 146–171. https://doi.org/10.1890/15-1027

Townsend, S. A., Webster, I. T., & Schult, J. H. (2011). Metabolism in a groundwater-fed river system in the Australian wet/dry tropics: Tight coupling of photosynthesis and respiration. *Journal of the North American Benthological Society*, 30(3), 603–620. https://doi.org/10.1899/10-066.1

Tweed, S., Leblanc, M., Bass, A., Harrington, G. A., Munksgaard, N., & Bird, M. I. (2016). Leaky savannas: The significance of lateral carbon fluxes in the seasonal tropics. *Hydrological Processes*, 30(6), 873–887. https://doi.org/10.1002/hyp.10640

van der Werf, G. R., Randerson, J. T., Giglio, L., Collatz, G. J., Mu, M., Kasibhatla, P. S., … van Leeuwen, T. T. (2010). Global fire emissions and the contribution of deforestation, savanna, forest, agricultural, and peat fires (1997–2009). *Atmospheric Chemistry and Physics*, 10(23), 11707–11735. https://doi.org/10.5194/acp-10-11707-2010

van der Werf, G. R., Randerson, J. T., Giglio, L., van Leeuwen, T. T., Chen, Y., Rogers, B. M., … Kasibhatla, P. S. (2017). Global fire emissions estimates during 1997–2016. *Earth System Science Data*, 9(2), 697–720. https://doi.org/10.5194/essd-9-697-2017

Vihermaa, L. E., Waldron, S., Domingues, T., Grace, J., Cosio, E. G., Limonchi, F., … Gloor, E. (2016). Fluvial carbon export from a lowland Amazonian rainforest in relation to atmospheric fluxes. *Journal of Geophysical Research: Biogeosciences*, *121*(12), 3001–3018. https://doi.org/10.1002/2016jg003464

Waterloo, M. J., Oliveira, S. M., Drucker, D. P., Nobre, A. D., Cuartas, L. A., Hodnett, M. G., … Múnera Estrada, J. C. (2006). Export of organic carbon in run-off from an Amazonian rainforest blackwater catchment. *Hydrological Processes*, *20*(12), 2581–2597. https://doi.org/10.1002/hyp.6217

Webb, J. R., Santos, I. R., Maher, D. T., & Finlay, K. (2019). The importance of aquatic carbon fluxes in net ecosystem carbon budgets: A catchment-scale review. *Ecosystems*, *22*(3), 508–527. https://doi.org/10.1007/s10021-018-0284-7

Whitley, R. J., Macinnis-Ng, C. M. O., Hutley, L. B., Beringer, J., Zeppel, M., Williams, M., … Eamus, D. (2011). Is productivity of mesic savannas light limited or water limited? Results of a simulation study. *Global Change Biology*, *17*(10), 3130–3149. https://doi.org/10.1111/j.1365-2486.2011.02425.x

Williams, R., Gill, A., & Moore, P. (1998). Seasonal changes in fire behaviour in a tropical savanna in northern Australia. *International Journal of Wildland Fire*, *8*(4), 227–239. https://doi.org/10.1071/WF9980227

Yan, J., Zhang, Y., Yu, G., Zhou, G., Zhang, L., Li, K., … Sha, L. (2013). Seasonal and inter-annual variations in net ecosystem exchange of two old-growth forests in southern China. *Agricultural and Forest Meteorology*, *182–183*, 257–265. https://doi.org/10.1016/j.agrformet.2013.03.002

Zeri, M., Sá, L. D. A., Manzi, A. O., Araújo, A. C., Aguiar, R. G., von Randow, C., … Nobre, C. A. (2014). Variability of carbon and water fluxes following climate extremes over a tropical forest in Southwestern Amazonia. *PLoS One*, *9*(2), e88130. https://doi.org/10.1371/journal.pone.0088130

Zhou, W.-J., Zhang, Y.-P., Schaefer, D. A., Sha, L.-Q., Deng, Y., Deng, X.-B., & Dai, K.-J. (2013). The role of stream water carbon dynamics and export in the carbon balance of a tropical seasonal rainforest, Southwest China. *PLOS One*, *8*(2), e56646. https://doi.org/10.1371/journal.pone.0056646

SUPPORTING INFORMATION

Additional supporting information may be found online in the Supporting Information section.